*Biochimica et Biophysica Acta*, 389 (1975) 1–12


BBA 76920

# CURRENT VOLTAGE CURVES OF BIMOLECULAR LIPID MEMBRANES

U. L. LÜSCHOW[a], K. D. HECKMANN[a] and M. PRING[b]

[a]*Lehrstuhl Chemie II, University of Regensburg, D-84 Regensburg, P.O. Box 397 (G.F.R.) and* [b]*Department of Biophysics, Medical School Computer Facility, University of Pennsylvania, Philadelphia, Pa. (U.S.A.)*

(Received December 24th, 1974)

## SUMMARY

The first part of this paper describes the current voltage curves of bimolecular membranes of oxidized cholesterol formed between two aqueous solutions of tetrabutylammonium chloride. These membranes are selectively permeable for cations and the membrane interfaces are electrically uncharged. The dependence of the membrane conductivity on the membrane potential can be described as the product of the conductivity at zero current ("zero conductivity") and a function called "overlinearity". The zero conductivity increases linearly with the concentration of tetrabutylammonium chloride. The overlinearity is independent of the concentration of tetrabutylammonium chloride.

In the second part the Nernst-Planck and Poisson equations are integrated numerically for a three-phase system consisting of an aqueous electrolyte solution, a membrane and an aqueous electrolyte solution. Each phase is characterized by material constants. Appropriate boundary conditions cause the electric current to build up electrical double layers on both sides of the membrane. The opposing double layers with opposite electrical signs inject the soluble ions into the membrane. This ion injection accounts for the overlinearity of the current voltage curves, thus explaining the measured characteristics.

## INTRODUCTION

Artificial lipid bilayer membranes resemble in thickness and in dielectric constant the lipid structures of biological membranes. In contrast to cell membranes, the artificial membranes allow a more direct investigation of certain properties. In particular, the penetration mechanisms of charged particles across lipid structures can be studied by applying electric and dielectric methods to artificial lipid bilayers and analysing their current voltage behavior. Because of the absence of carrier molecules and pore structures in pure artificial lipid bilayer membranes, the simple diffusion and migration mechanisms may be investigated in this fashion, whereas in biological membranes these processes are obscured by more complicated phenomena.

We were interested in the penetration of a uni-uni-valent electrolyte across

electrically neutral lipid bilayer membranes, under the special condition that the transference number of one of the ion species is nearly one. As electrolyte we therefore chose tetrabutylammonium chloride*, which consists of one hydrophilic and one lipophilic ion; as lipid we used oxidized cholesterol which, although chemically not very well defined, bears no electric net charge and produces stable membranes (mean life time approx. 60 min).

The measured electrical characteristics of these membranes can be explained by integrating the differential equations of Nernst-Planck and Poisson. The integration and the determination of boundary conditions convert these equations into a phenomenological model for the system aqueous solution-membrane-aqueous solution. Such models with locally independent constants have been repeatedly described [7–9]. However, their ability to explain the electrical characteristics of thin lipid membranes was questioned [9], since they did not exhibit the strong overlinearity of the current voltage curves found experimentally.

In contrast to other authors, we have chosen a finite extension of the aqueous phases and finite ion conductivities within the aqueous phases. We have also chosen boundary conditions which enable the electric current across the membrane to build up electric charges at the membrane surfaces.

## MEMBRANES OF OXIDIZED CHOLESTEROL BETWEEN AQUEOUS SOLUTIONS OF TETRABUTYLAMMONIUM CHLORIDE

### *Methods*

Oxidized cholesterol** was produced according to Tien et al. [1] by oxidizing a dispersion of cholesterol*** in water with molecular oxygen at 98 °C, and by repeatedly recrystallizing the product in ethanol. This procedure yields a mixture of approximately 5 % keto- and hydroxycholesterol and 95 % cholesterol.

The measuring cell is shown in Fig. 1. It consists mainly of two teflon chambers bolted to one another. This arrangement protects the fragile membranes from pressure and volume fluctuations of the outer solution and allows for a one-sided ex-

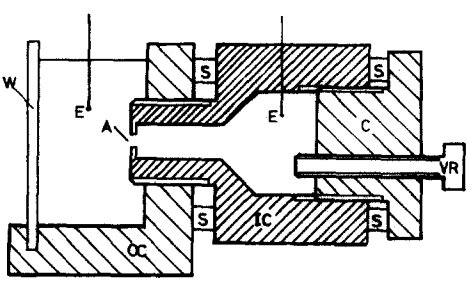


Fig. 1. Measuring cell: OC, outer chamber; C, closing; W, window; VR, volume regulation; A, aperture; S, sealing; IC, inner chamber; E, electrodes.

* Tetra-*n*-butylammonium chloride for polarography; K. Roth, D-75 Karlsruhe.

** Kindly supplied by B. Dobias, Department of Chemistry, University of Regensburg.

*** Cholesten-(5)-ol-(3) $C_{27}H_{46}O$ Cod. France; Merck, D-61 Darmstadt.

change of solutions within 1–2 s. This exchange of solutions is so fast that changes in membrane properties, due to ageing processes during this procedure, can be neglected.

The membranes were formed by brushing a solution of oxidized cholesterol (15 mg dissolved in 1 ml octane) on the aperture of the inner chamber.

The stationary current voltage curves were measured using a potentiometer (Keithley 602) under current clamp conditions. They were recorded on a compensation plotter. In order to measure the diffusion potentials, the original solution in the outer chamber was successively replaced after forming the membranes by other solutions of differing tetrabutylammonium chloride concentrations.

*Measurements*

The membranes turned black after 1 min. Their electrical resistance decreased in time $t$ and was nearly constant after 15 min. No electrical property recorded here was measured before $t = 15$ min.

The electrical capacity of the membranes was found to be 0.35 $\mu F \cdot cm^{-2}$. Assuming the dielectric constant to be 2 and the membrane to behave as a plate capacitor, we calculated a membrane thickness of 50 Å [2, 3].

For a concentration ratio $c'/c'' = 0.1$ and for $10^{-4} \leqslant c' \leqslant 10^{-2}$ mol $\cdot l^{-1}$, the diffusion potential $V_d$ at zero current ranges from 55 to 57 mV. Inserting this value into the Goldman equation* we find the permeability ratio $P_{TBA^+}/P_{Cl^-} > 33$, where $P_{TBA^+}$ refers to the permeability of the tetrabutylammonium ion.
For equal concentrations $c' = c'' = c$ on both sides of the membrane, we find current voltage curves (Fig. 2) similar to those reported by other authors (e.g. refs 4 and 6).

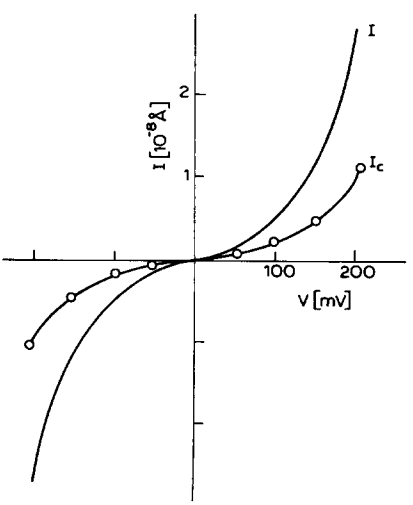


Fig. 2. Measured $I$-$V$ curves with $c = 10^{-3}$ mol $\cdot l^{-1}$. $I_c$ curve (marked with ○) is one single continuous recording. $I$ curve is an average of 15 continuous recordings. Maximum deviation from mean value $\Delta I = 3 \cdot I$.

* Goldman equation [5]:

$$V_d = -RT/F \cdot \ln \frac{P_{Cl^-} \cdot c'_{Cl^-} + P_{TBA^+} \cdot c''_{TBA^+}}{P_{Cl^-} \cdot c''_{Cl^-} + P_{TBA^+} \cdot c'_{TBA^+}}$$

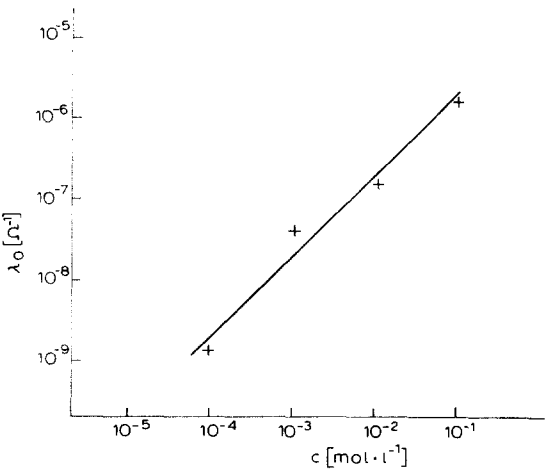


Fig. 3. Measured zero conductivity $\lambda_0$ as a function of $c$. Maximum deviation $\Delta\lambda_0 = 3 \cdot \lambda_0$. Points are averages of 15 measurements.

In the potential range $V < 25$ mV the current increases approximately linearly. With increasing potential, in the range $V > 25$ mV, the increase is more than linear.

In order to describe this behavior quantitatively, a function $f(V)$ (overlinearity) is defined,

$$f(V) = \frac{\lambda(V)}{\lambda_0}$$

where $\lambda(V) = I(V)/V$ is the conductivity at voltage $V$, and $\lambda_0 = dI(o)/dV$ is the conductivity extrapolated to zero current (zero conductivity). The introduction of this function allows us to write the electrical current in the form $I(V) = \lambda_0 \cdot f(V) \cdot V$ and to express the conductivity by the product

$$\lambda(V) = \lambda_0 \cdot f(V).$$

The overlinearity was found to be independent of the tetrabutylammonium chloride concentration and highly reproducible (Figs 3 and 4). The zero conductivity is only poorly reproducible from one experiment to the next. It is approximately linearly dependent upon the tetrabutylammonium chloride concentration*.

In the following chapter we attempt to calculate current voltage curves by integrating the Nernst-Planck equations and the Poisson equation and to fit these calculated curves to the measured data.

## INTEGRATION OF THE NERNST-PLANCK AND POISSON EQUATIONS

### *Differential equations*

Symbols: $F$, $R$, $T$, $\varepsilon_v$, $\varepsilon_0$ are: Faraday constant, gas constant, temperature,

* The same behavior was found by R. Brennecke (6) using the same membrane system but different electrolytes.

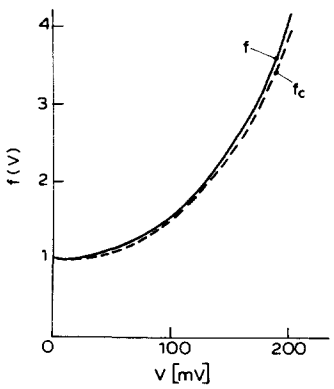


Fig. 4. Measured overlinearity f($V$). $f_c$ curve (dotted) is the overlinearity of the single $I_c$ curve in Fig. 2 with $c = 10^{-3}$ mol · l$^{-1}$. $f$ is an average of the calculations. $10^{-4} \leqq c \leqq 10^{-2}$ mol · l$^{-1}$. Maximum deviation is $\Delta f(V) < 0.1 \cdot f(V)$.

relative and absolute dielectric constant, and $\nu = 1, 2, 3$ indicates the three phases: aqueous solution, membrane, aqueous solution.

$x$ = position
$n_\nu^\pm(x)$ = concentration of the respective cation or anion
$u_\nu^\pm$ = mobility of the respective cation or anion
$k^\pm$ = distribution coefficient of the respective cation or anion
$j^\pm$ = current density of the respective cation or anion
$j(V) = j^+ - j^-$, total current density
$Q$ = membrane area
$I = Q \cdot F \cdot j$, electrical current
$\lambda(V) = I(V)/V$, electrical conductivity
$\lambda_0 = \mathrm{d}I(\mathrm{o})/\mathrm{d}V$, zero conductivity
$\mathrm{f}(V) = \lambda(V)/\lambda_0$, overlinearity
$\Psi_\nu(x)$ = electrical potential
$V$ = voltage between the electrodes
$c$ = ion concentration at both electrodes
$d_\nu$ = extension of phase $\nu$
$\alpha_{\mathrm{l,r}}$ = surface charge at the left or right membrane boundary, respectively.
$\alpha_\nu^\pm = 1/(u_\nu^\pm \cdot R \cdot T)$
$\beta = F/(R \cdot T)$
$\gamma_\nu = F/(\varepsilon_\nu \cdot \varepsilon_0)$
$\mathrm{f}'(x) = \mathrm{d}f(x)/\mathrm{d}x$

In order to describe each of the three phases, including its extension, five material constants are required (chemical potentials and mobilities of the respective cations and anions and dielectric constants). We made the simplifying assumption that, in each of the phases, the material constants are independent of position, field strength, and concentrations, and that at the phase boundaries of the membrane, the constants show discontinuities.

For monovalent cations and anions the one-dimensional form of the Nernst-

Planck and the Poisson equations can be written as

$$\begin{aligned} n_\nu^{\pm\prime}(x) &= -j_\nu^{\pm} \cdot \alpha_\nu^{\pm} \mp n_\nu^{\pm}(x) \cdot \psi_\nu'(x) \\ \psi_\nu'(x) &= -\gamma_\nu \cdot (n_\nu^{+}(x) - n_\nu^{-}(x)). \end{aligned} \qquad \nu = 1, 2, 3 \tag{1}$$

In this formulation, a steady state is characterized by the constancy of the ion currents with respect to $x$.

This system of six first-order and three second-order differential equations contains six unknown parameters ($j_\nu^{\pm}$, $\nu = 1, 2, 3$) and requires 18 boundary conditions for its solution.

*Boundary conditions*

The boundary conditions (C1–C18) are determined by the following assumptions:

C1–C6: Constancy of the total current, of the ion concentrations at the electrodes, and of the electrical potential of the electrolyte solution at one electrode.

C7–C16: Continuity of ion currents, electrical potential and chemical potentials.

C17: Total electroneutrality: the electrodes do not charge the three-phase system.

C18: In the case of zero current: the membrane surfaces bear no fixed charges. In the case of non-zero current: the current can build up surface charges of opposite signs ($\sigma_l = -\sigma_r$) at both membrane boundaries.

The continuity of the electrical potential and the chemical potentials in the phase boundaries results in an ion distribution between water and lipid which is described by ion distribution coefficients $k^{\pm}$. For a symmetrical membrane, the electrical potential can be assumed to be continuous even in the presence of dipoles in the interfaces, because the two resulting potential jumps compensate one another.

Electrical charges at infinity do not determine the potential at a finite position. Therefore, the total electroneutrality (C17) is meaningless in a theoretical three-phase system with infinitely extending aqueous phases. Assuming a finite extension of the aqueous phases, the boundary conditions C1–C17 cause the electric current to build up charges at the membrane interfaces. Condition C18 reflects the symmetry of the three-phase system.

Eqn 1 can only be integrated in closed form for infinitely extending aqueous phases [12]. The restriction of finitely extending aqueous phases excludes an integration in closed form for any of the three phases.

*Numerical integration*

The differential equations were integrated numerically using the Cauchy-Heun [13] procedure:

$$f_\mu(x+\Delta x) = f_\mu(x) + \{3 \cdot f_\mu'(x+2 \cdot \Delta x/3) + f_\mu'(x)\} \cdot \Delta x/4 + R_\mu(x)$$

with

$$R_\mu \leqq \{f_\mu'(x+2 \cdot \Delta x/3) \cdot 3/2 - f_\mu'(x+\Delta x) - f_\mu(x)/2\} \cdot \Delta x$$

and

$$f_1(x) = n_\nu^+(x) = \int (-j_\nu^+ \cdot \alpha_\nu^+ - n_\nu^+(x) \cdot \Psi_\nu'(x)) \cdot dx$$

$$f_2(x) = n_\nu^-(x) = \int (-j_\nu^- \cdot \alpha_\nu^- + n_\nu^-(x) \cdot \Psi_\nu'(x)) \cdot dx$$

$$f_3(x) = \Psi_\nu'(x) = \int (-\gamma_\nu \cdot (n_\nu^+(x) - n_\nu^-(x)) \cdot dx$$

$$f_4(x) = \Psi_\nu(x) = \int f_3(x) \cdot dx \qquad \nu = 1, 2, 3$$

This integration procedure is relatively simple and indifferent to rounding errors and it allows for varying the step length of the integration by testing the remainder $R_\mu$.

The 18 boundary conditions are of such a nature that three of them (C4, C5, C17) cannot be explicitly fulfilled. Only by calculating the deviations*:

$$dev_A = (n_3^+(x_3) - c_1)/c_1$$
$$dev_B = (n_3^-(x_3) - c_1)/c_1$$
$$dev_C = (\Psi_3'(x_3) - \Psi_1'(x_0))/\Psi_1'(x_0)$$

and the square error

$$SQR = dev_A^2 + dev_B^2 + dev_C^2$$

and by minimizing this error SQR can these conditions be solved.

According to this nature, there are three boundary values:

$$BDV(1) = \Psi_1'(x_0)$$
$$BDV(2) = \Psi_2'(x_1)$$
$$BDV(3) = j^+$$

which have to be arbitrarily interpolated before the first integration process is started. The square error SQR is a function of the above values.

After each integration cycle, the program (flow chart in Fig. 10) improves the boundary values by minimizing the error function until SQR $<$ MUST. It was necessary to choose the threshold MUST $< 10^{-6}$ in order to obtain results with an accuracy of 1 %.

*Solutions of the equations*

The material constants of the aqueous phases

$$\alpha_1^+ = \alpha_3^+ = 22 \cdot 10^4 \text{ s} \cdot \text{cm}^{-2} \qquad \varepsilon_1 = \varepsilon_3 = 78$$
$$\alpha_1^- = \alpha_3^- = 55 \cdot 10^3 \text{ s} \cdot \text{cm}^{-2} \qquad \beta = 38\ V^{-1}$$

---

* $x_0$ is the $x$ value for the left boundary of phase 1 (left water phase); $x_1$ is the $x$ value for the left boundary of phase 2 (membrane); $x_3$ is the $x$ value for the right boundary of phase 3 (right water phase).

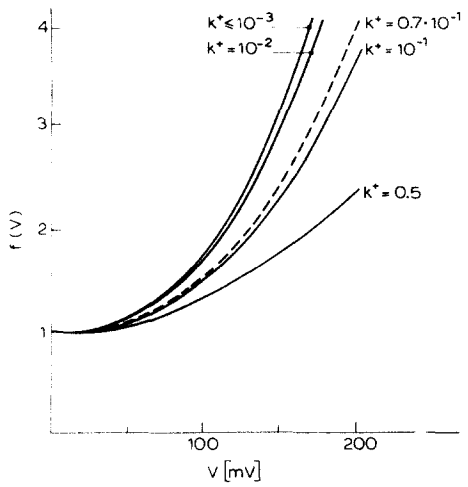


Fig. 5. f($V$) for different values of the distribution coefficient $k^+$ with $c = 10^{-3}$ mol · l$^{-1}$. The measured curve (dotted) can be fitted using $k^+ = 0.7 \cdot 10^{-2}$.

and the membrane constants

$$\varepsilon_2 = 2 \qquad\qquad d_2 = 5 \cdot 10^{-7} \text{ cm}$$

were obtained from the literature [2, 3, 5, 14].

Under the conditions $\alpha_1^{\pm} \leqq 0.1 \cdot \alpha_2^{\pm}$ and $d_1 = d_3 > d_2$ the calculated current voltage curves were found to be essentially independent of the ion mobilities in water and of the extension of the aqueous phases.

For each voltage, the ion currents were found to be proportional to the functions $k^{\pm} \cdot c/\alpha_2^{\pm}$.

The overlinearity f($V$) increases continuously if $k^+$ is decreased from 0.5 to $10^{-3}$ at a constant concentration. At $k^+ \leqq 10^{-3}$, f($V$) approaches a limit (Fig. 5). At concentration $c = 10^{-3}$ mol · l$^{-1}$, the experimental curve is fitted perfectly by choosing $k^+ = 0.7 \cdot 10^{-1}$. However, for this value of the distribution coefficient and all other $k^+ > 10^{-3}$, the calculated f($V$) is concentration dependent (Fig. 6),

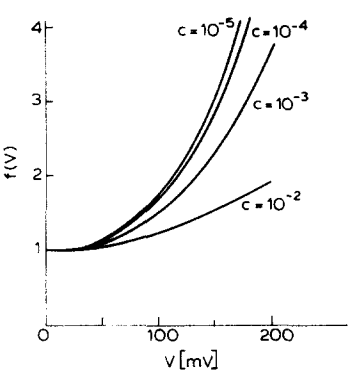


Fig. 6. f($V$) for different values of the concentration $c$ (mol · l$^{-1}$) with $k^+$ = 0.1.

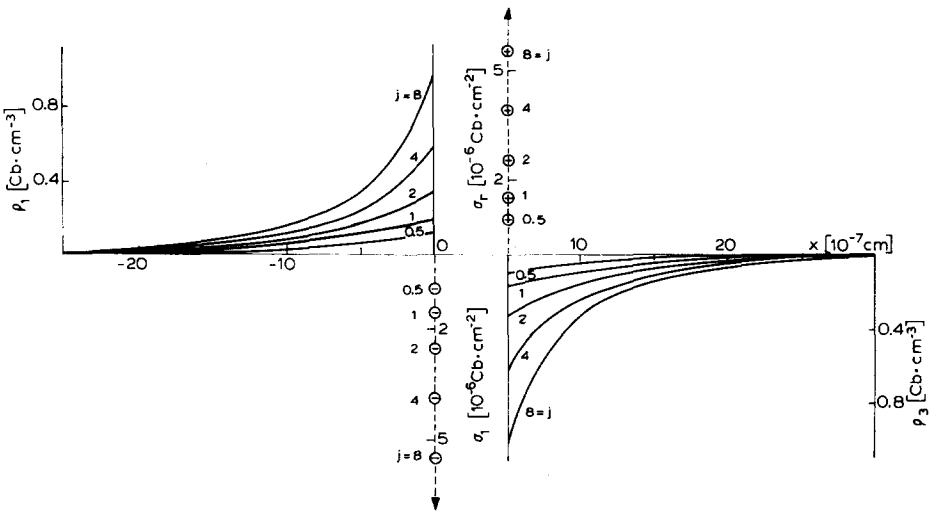


Fig. 7. Surface charges $\sigma_l$ and $\sigma_r$ and space charge density $\rho_v(x)$ for different values of the total current density $j$ ($10^{-13}$ mol · s$^{-1}$ · cm$^{-2}$) with $c = 10^{-3}$ mol · l$^{-1}$. Cations are moving from left to right.

in contrast to the experimental results. $f(V)$ is independent of concentration only for $k^+ \leqq 10^{-3}$ and in the range of $10^{-5} \leqq c \leqq 10^{-2}$ mol · l$^{-1}$. Under these conditions the calculation yields the experimentally found equation

$$\lambda(V) = \lambda_0 \cdot f(V),$$

whose factors show the measured characteristics: $\lambda_0$ is proportional to concentration and independent of voltage; $f(V)$ is independent of concentration and dependent upon voltage.

An optimum fit is found for

$$k^+ \leqq 10^{-3} \qquad k^- < 10^{-2} \cdot k^+$$

$$k^+/\alpha_2^+ = 57 \cdot 10^{-10}/\alpha_1^- \qquad \alpha_2^- = 10^4 \cdot \alpha_1^-$$

For this set of constants the measured dependence of the zero conductivity, $\lambda_0$, to

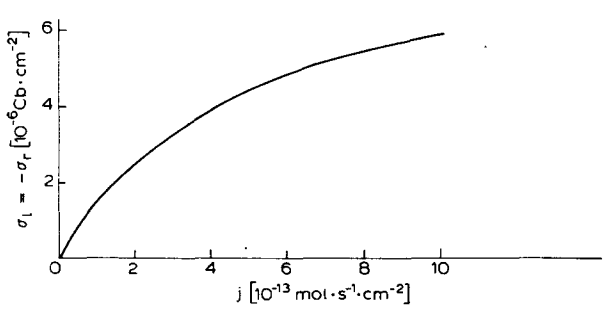


Fig. 8. Dependence of the surface charges $\sigma_l = -\sigma_r$ upon the current density with $c = 10^{-3}$ mol · l$^{-1}$.

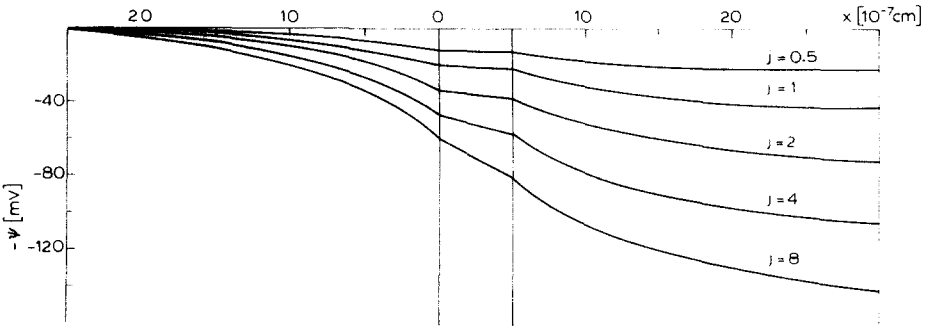


Fig. 9. Potential profile for different values of the current density $j$ ($10^{-13}$ mol · s$^{-1}$ · cm$^{-2}$) with $c = 10^{-3}$ mol · l$^{-1}$.

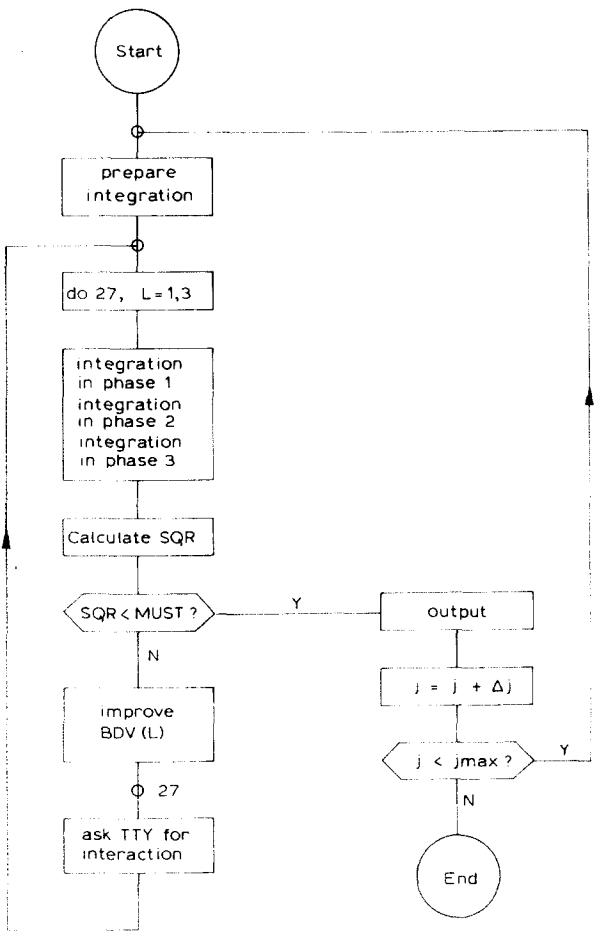


Fig. 10. Simplified flow chart of the program. For comments, see the section Numerical integration.

concentration (Fig. 3) can be exactly reproduced. However, the calculated overlinearity $f(V)$ is somewhat greater than measured. The difference between the calculated and the measured overlinearity is the difference between the curve with $k^+ < 10^{-3}$ and the (dotted) curve with $k^+ = 0.7$ in Fig. 5. The total current density $j$ is dependent upon $\varepsilon_1$, $\beta$ (hence temperature), $k^+$ and $V$, but independent of $a_2^-$, $k^-$ (since $j^+ \gg j^-$) and $\varepsilon_2$.

Figs 7 and 8 reflect the current dependence of the local space charge and the surface charges: the current builds up electrical double layers on either side of the membrane, each of them consisting of a surface charge at the membrane boundary and of a diffuse space charge in the adjacent aqueous phase. Unexpectedly, the main part of the electrical potential does not drop inside the membrane, but within the double layers, where the maximum field strengths are also found (Fig. 5).

## DISCUSSION

The results of our calculation show that the experimentally determined behavior of the membrane system can be described entirely by phenomenological considerations, and they indicate a mechanism that might be responsible for the overlinearity of current voltage curves. The discrepancies between measurements and calculations found for higher currents may be eliminated by simply assuming that the membrane parameters ($\varepsilon_2$, $u_2^+$, $k_2^{\pm}$, $d_2$) depend upon concentration and/or field strength. According to the mechanism suggested, the overlinearity of the current voltage curves is explained by current-dependent double layers. The formation of these double layers implies an enrichment of cations and a depletion of anions in front of one membrane surface and the opposite effect in front of the other surface. These changes of the ion concentration in the aqueous phases are, via the ion distribution coefficient, coupled to similar changes inside the membrane, which in turn lead to increased ion concentration gradients across the membrane. Since the total current inside the membrane is mainly (approx. 90%) determined by the diffusion of the cation ($j_d^+ = -u^+ \cdot R \cdot T \cdot n^{+\prime}(x)$) as shown by the calculation, the increase in the cation concentration gradient between the membrane boundaries leads to an increased cation current and hence to an increased total current. In short, our calculations suggest a current-induced increase in current ("ion injection" [9]).

This result was obtained because we did not a priori forbid the existence of surface charges. Consequently, our calculations postulate the current-induced existence of surface charges without, however, commenting on the nature of these charges.

The surface charges may be caused by the adsorption of mobile ions and/or by a polarisation of membrane material.

The origin of the surface charges, nearly compensated by the space charges in the adjacent aqueous phases, can be macroscopically interpreted as follows: in a non-steady state, the ion currents are discontinuous at the membrane boundaries because of the discontinuity of the material constants. Thus, electric charge is assembled at the interfaces, until the process becomes stationary and the currents are continuous everywhere [10, 11].

ACKNOWLEDGEMENTS

We want to thank Professor Dr H. Passow for valuable discussions and helpful assistance. The paper was supported by the Deutsche Forschungsgemeinschaft (Lu 161).

REFERENCES

1 Tien, H. T., Carbone, S. and Dawidowicz, E. A. (1966) Nature 212, 718–719
2 Tien, H. T., Carbone, S. and Dawidowicz, E. A. (1966) Kolloid-Z. Polymere 212, 165–166
3 Tien, H. T. and Dawidowicz, E. A. (1966) J. Coll. Interf. Sci. 22, 438–453
4 Walz, D., Bamberg, E. and Läuger, P. (1969) Biophys. J. 9, 1150–1159
5 Goldman, D. E. (1943) J. Gen. Physiol. 27, 37–60
6 Brennecke, R. (1970) Dissertation, Universität Saarbrücken
7 Bruner, L. J. (1965) Biophys. J. 5, 867–908
8 Eisenman, G., Ciani, S. M. and Szabo, G. (1968) Fed. Proc. 27, 1289–1304
9 Walz, D., Bamberg, E. and Läuger, P. (1969) Biophys. J. 9, 1150–1159
10 Hund, F. (1956) Theoretische Physik, Vol. II, pp. 83–88, Teubner Verlagsges., Stuttgart
11 Becker, R. and Sauter, F. (1964) Theor. Elektr. 1, pp. 104–106, Teubner Verlagsges., Stuttgart
12 Overbeek, J. Th. G. (1952) Coll. Sci. 1, 128–132
13 Berezin, I. S. and Zhidow, N. P. (1965) Computing Methods, Vol. II, pp. 310–320, Pergamon Press, New York
14 Landolt-Börnstein (1960) Zahlenwerte und Funktionen (Bartels, J., ed.), Vol. II, 7, pp. 258–266, Springer-Verlag, Berlin